

Critical properties of the random dipolar-coupled ferromagnet $\text{LiTb}_p\text{Y}_{1-p}\text{F}_4$

J. J. Folkins* and J. A. Griffin

*Department of Physics and Laboratory for Research on the Structure of Matter,
University of Pennsylvania, Philadelphia, Pennsylvania 19104*

D. U. Gubser

Naval Research Laboratory, Washington D. C. 20375

(Received 24 August 1981)

The critical properties and the critical temperature T_c versus concentration p phase diagram of a site-diluted long-range coupled magnet have been measured and compared with renormalization group (RG) and $T_c(p)$ predictions. Zero-field magnetic-susceptibility measurements for eight concentrations p of the randomized dipolar-coupled Ising ferromagnet $\text{LiTb}_p\text{Y}_{1-p}\text{F}_4$ have been found to be inconsistent with "universal" RG predictions made for this system. The fact that subsequent "nonuniversal" RG theories have been shown to agree with the data suggests that the asymptotic reduced temperature range cannot be attained in this system. The effective susceptibility critical exponents γ are found to be p dependent. The T_c -vs- p phase line has been found to be linear for the entire concentration range measured with an extrapolated percolation concentration $p_c=0.12$. This behavior is in contrast to short-range coupled magnets.

I. INTRODUCTION

Whereas the critical behavior of the pure dipolar-coupled Ising ferromagnet is one of the best understood problems in critical phenomena, the introduction of random impurities into this system considerably complicates the problem. Owing to a general argument by Harris,¹ as well as subsequent renormalization group (RG) calculations,² a crossover to a new type of critical behavior is expected in a randomized magnet if the specific heat diverges at T_c in the pure material. In this paper we report on the critical properties of the magnetic susceptibility of the randomized dipolar-coupled Ising ferromagnet $\text{LiTb}_p\text{Y}_{1-p}\text{F}_4$. The properties have been determined by measuring the zero-field magnetic susceptibility in the critical regions above $T_c(p)$ for eight concentrations p in the range $0.155 \leq p \leq 0.97$. We find that the susceptibility exhibits nonuniversal behavior with concentration-dependent effective exponents γ . The ferromagnetic-paramagnetic $T_c(p)$ phase diagram for a randomized dipolar-coupled Ising ferromagnet has been mapped out and found to be linear in the range $p \geq 0.155$.

II. THEORETICAL MOTIVATION

A. Marginal dimensionality and random systems

Systems near their critical points are characterized by a marginal dimensionality d^* . If

the dimensionality d of the system is larger than d^* , the critical phenomena of the system is described by mean-field theories with classical critical-point exponents. However, d is greater than d^* in few if any systems. If $d < d^*$ the RG recursion relations are solved for the critical exponents in terms of a power series in the parameter $\epsilon = d^* - d$. These asymptotic series have poor convergence properties. If $d = d^*$, the RG recursion relations are solved "exactly" resulting in predictions for logarithmic corrections to the mean-field behavior.³ Because of the well-defined analytic behavior of these logarithmic expansions, measurements in systems in which $d = d^*$ provide more stringent tests for RG theories than systems in which $d < d^*$. The marginal dimensionality d^* depends upon the type of critical point and the type and dimension of the ordering interactions. One of the few systems which exhibits a physically accessible d^* is the long-range dipolar-coupled Ising ferromagnet for which $d^* = d = 3$. Loosely speaking, a dipolar Ising ferromagnet has $d^* = 3$ instead of $d^* = 4$, as is the case in most magnetic systems, because the dipolar forces suppress longitudinal fluctuations of the spin. The Ising behavior does not allow the transverse spin components to pick up the fluctuation strength,³ fluctuations are suppressed, and hence d^* is reduced.

The behavior in the critical region of several

thermodynamic functions has been calculated. The magnetic susceptibility predicted at the marginal dimensionality in the dipolar Ising magnet is given by⁴

$$\chi \propto t^{-1} |\ln t|^{1/3} \left[1 + \left(\frac{1}{3}\right)^5 (108 \ln \frac{4}{3} + 41) \times \frac{\ln |\ln t|}{|\ln t|} + O\left(\frac{1}{|\ln t|}\right) \right]^{-1} \quad (1a)$$

or

$$\chi = \Gamma t^{-1} [\ln(t_0/t)]^{1/3}, \quad (1b)$$

where we have included the parameter t_0 in Eq. (1b) to account for the higher-order logarithmic corrections in Eq. (1a) and $t = (T - T_c)/T_c$ is the reduced temperature. Previous heat capacity,⁵ neutron diffraction,⁶ light scattering,⁷ and magnetization⁸ experiments with dipolar Ising magnets have confirmed the validity of the logarithmic corrections to mean-field behavior predicted by such RG calculations.

In 1976 Aharony used RG techniques to treat the problem of randomization at $d = d^*$ for a dipolar Ising magnet.⁹ In the randomization problem, a fraction $1 - p$ of the magnetic ions is replaced by nonmagnetic ions. A crossover from the critical-behavior equation (1) to a new type of critical behavior given by^{9,10}

$$\chi = \Gamma t^{-1} \exp\{ [D \ln(t_0/t)]^{1/2} \}, \quad (2)$$

where $D = 0.11795 \dots$ is a universal number, and where t_0 is inserted to account for the higher-order corrections. This crossover occurs for reduced temperatures much smaller than a crossover temperature t_x given by $\ln(t_x) \propto -g(0)/[p(1-p)\eta^2]^3$, where $g(0)$ is the ratio of the dipolar to exchange coupling, η is the shift in the mean-field critical temperature, and p is the magnetic site occupation probability. Since we cannot determine all of the constants in this equation we are unable to estimate the numerical value of t_x .

Because of the uncertainty of the actual magnitude of the reduced temperature "crossover region" separating the regions of the universal behavior equations (1) and (2), Vause and Bruno¹¹ have taken the "random" recursion relations⁹ and solved them to a lower order obtaining a nonuniversal susceptibility appropriate in the exterior region

$t_x \ll t$. This form is given as

$$\chi = \Gamma t^{-(1+\lambda/6)} R^{1/3} \times \exp\left\{ -\frac{1}{2}(\lambda/2)[R^{1/3} - (\ln t_0)^{1/3}] \right\}, \quad (3)$$

$$R \equiv 2/\lambda + (\ln t_0 - 2/\lambda)t^{\lambda/2},$$

where λ and t_0 are nonuniversal parameters. λ is predicted to depend on p as $\lambda \propto (1-p)^3$. In the limit $\lambda \rightarrow 0$ ($p \rightarrow 1$), Eq. (3) and the pure universal RG form Eq. (1) are the same, with Γ and t_0 having the same meanings in both forms. In the large λ small t limit $t^\lambda \ll 1$, Eq. (3) has the same functional form as the conventional critical exponent power law given by

$$\chi = \Gamma t^{-\gamma}, \quad (4)$$

where the critical exponent γ is related to λ by $\gamma - 1 = \lambda/6$ and the Γ 's are trivially related using t_0 and λ .

For $p = 1$ the "pure" universal susceptibility equation (1) is strictly true for all t within the "critical region"³ [the upper bound of the critical region has generally been found to be about $t = 10^{-1}$ in LiTbF₄ (Refs. 5–8)]. For $p < 1$ the magnetic susceptibility given by the nonuniversal equation (3) describes the system. However, when the reduced temperature becomes smaller than some crossover temperature t_x , the RG recursion relations "flow" to a new fixed point, causing a crossover to the new universal critical behavior equation (2). A schematic representation of the crossover region separating the universal random behavior equation (2) from the nonuniversal random behavior equation (3) is shown in Fig. 1.

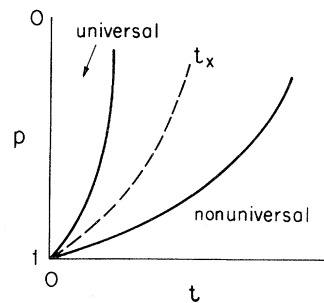


FIG. 1. Schematic representation of the crossover region separating the universal random RG prediction equation (2) and the nonuniversal random RG predictor equation (3).

B. T_c -vs- p phase diagram

Ferromagnetic phase transition diagram measurements $T_c(p)$ have not previously been made for a randomized dipolar-coupled magnet. $T_c(p)$ of the short-range exchange-coupled magnet has been studied theoretically in quite some detail.^{1,2,12} In the short-range case, the phase line is linear in p near $p = 1$, it then deviates from this linearity by passing through $T_c(p_c) = 0$ at a finite percolation concentration p_c . A mean-field coupled magnet (i.e., infinite range coupled) exhibits a linear phase line for all p , with a slope $dT_c(p)/T_c(1)dp$ of one, which passes through $T_c(p_c = 0) = 0$. The $1/r^3$ dipolar interactions might be expected to exhibit $p_c = 0$ because of their long-range nature. Stephen and Aharony¹³ have studied the quenched bond dilute dipolar-coupled Ising model using a replica trick method. They have concluded that indeed $p_c = 0$ and that the $T_c(p)$ phase line should be given to first order in p by the relation

$$1 = p \sum_i \tanh(J_{ij}/kT_c), \quad (5)$$

where the dipole interactions J_{ij} are given by

$$J_{ij} = \frac{g^2 \mu_B^2}{4r_{ij}^3} [3(Z_{ij}/r_{ij})^2 - 1] \quad (6)$$

and where the summation is over the Tb or Y ion sites. Beauvillain *et al.*¹⁴ have performed a series expansion of $(\chi T)^{-1}$ in powers of T^{-1} for a site randomized dipolar-coupled Ising ferromagnet, obtaining

$$1 = p \sum_i \tanh(J_{ij}/kT_c) + pS/kT_c + \sigma(P/kT_c)^2, \quad (7)$$

where $\sigma \equiv \sum_i J_{ij}^2$ and S is used as an adjustable parameter. The range of applicability for the replica prediction equation (5) is small p and low temperatures, whereas for the series expansion prediction equation (7) this range is for large p and high temperatures.

III. $\text{LiTb}_p\text{Y}_{1-p}\text{F}_4$

LiTbF_4 is colorless and optically clear. It has the crystal structure of mineral scheelite CaWO_4 (space group $C_{4h}^6 - I4_1/a$).^{15,16} There are four Tb^{3+} ions in each body-centered tetragonal unit cell with $c = 10.87 \text{ \AA}$ and $a = 5.18 \text{ \AA}$. The ground configuration of the free Tb^{3+} ion is $4f^8$. The spin-

orbit perturbation yields a 7F_6 ground term. Each Tb^{3+} ion is located on a site of S_4 crystal-field symmetry which splits the 7F_6 term into ten levels. The lowest states are two nearly degenerate Γ_2 levels, and the first excited state is a $\Gamma_{3,4}$ doublet lying 150 K above the ground states.¹⁶ The Γ_2 levels produce the effective spin- $\frac{1}{2}$ Ising magnetic behavior (with $g_{||}/g_{\perp}$ nearly infinite) in LiTbF_4 . The $4f$ electrons have very little exchange coupling to the neighboring Tb^{3+} ions, which leads to the predominance of dipolar over exchange coupling in LiTbF_4 . The exchange contributions to T_c are measured to be only about 10% of the dipolar contributions.¹⁷ Thus, in LiTbF_4 the Tb^{3+} ions produce Ising doublet magnetic moments which couple to each other primarily through their dipolar rather than their exchange interactions. LiTbF_4 has been used as a model system in which to study the marginal dimensionality RG predictions made for a long-range dipolar-coupled Ising ferromagnet.^{5-8,15,17}

LiYF_4 has the CaWO_4 structure with $a = 10.74 \text{ \AA}$ and $c = 5.18 \text{ \AA}$. The random mixture $\text{LiTb}_p\text{Y}_{1-p}\text{F}_4$ crystallizes for the entire $0 \leq p \leq 1$ concentration range. Because Y^{3+} has the non-magnetic, closed $4p^6$ ground configuration, these mixed crystals represent a model system for the randomized, dipolar-coupled, Ising ferromagnet.^{9,14,18}

The Tb^{3+} ground-state Γ_2 levels are actually split by $\Delta = 1.3 \text{ K}$ by a crystal field which is formally equivalent to a magnetic field applied transverse to the spin axis.^{19,20} RG as well as series expansion methods have predicted that for splittings less than some critical value the critical exponents should be unaffected.²¹ Because of these results, the splitting will not be considered further with regard to the critical region susceptibilities. A mean-field calculation^{20,22} for the Curie-Weiss temperature in a random magnet with a split ground state indicates that $T_c(p)$ will be affected by the splitting. The 1.3-K splitting in LiTbF_4 is calculated to increase the slope $dT_c(p)/T_c(1)dp$ by approximately 5% for $p \geq 0.4$ and then to cause $T_c(p)$ to fall to zero at $p = 0.23$.

IV. EXPERIMENTAL

A. Crystal preparation

Eight single crystals of $\text{LiTb}_p\text{Y}_{1-p}\text{F}_4$ with different concentrations p were used in these experiments. The crystals were grown in an inert argon

TABLE I. Results from the least-square fits of the critical-behavior predictions to the magnetic susceptibility of $\text{LiTb}_p\text{Y}_{1-p}\text{F}_4$. The susceptibilities are in cm^3/g and have been corrected for demagnetizing effects. All of the fits had the same number of adjustable parameters.

	Concentration p	0.97 ± 0.015	0.90 ± 0.015	0.79 ± 0.02
	Density (g/cm^3)	5.42 ± 0.02	5.31 ± 0.02	5.16 ± 0.05
	Temperature range	$9 \times 10^{-4} < t < 10^{-1}$	$9 \times 10^{-4} < t < 10^{-1}$	$4 \times 10^{-3} < t < 10^{-1}$
Equation (2)	T_c (K)	2.7682	2.5552	2.2108
Random RG		± 0.0004	± 0.0004	± 0.0006
$\Gamma t^{-1} \exp\{[D \ln(t_0/t)]^{1/2}\}$	t_0	3.0 ± 1.0	2.5 ± 1.0	0.47 ± 0.20
	Γ ($10^{-2} \text{cm}^3/\text{g}$)	3.28 ± 0.15	3.52 ± 0.15	4.68 ± 0.20
	χ^2	1.4	1.3	2.3
Equation (1)	T_c (K)	2.7686	2.5556	2.2112
Pure RG		± 0.0004	± 0.0005	0.0006
$\Gamma t^{-1} [\ln(t_0/t)]^{1/3}$	t_0	3.0 ± 1.0	2.9 ± 1.0	1.0 ± 0.2
	Γ ($10^{-2} \text{cm}^3/\text{g}$)	4.09 ± 0.10	4.34 ± 0.10	5.39 ± 0.16
	χ^2	1.5	1.7	2.8
Equation (3)	T_c (k)	2.7681	2.5551	2.2101
Crossover region		± 0.0006	± 0.0006	± 0.0009
$\Gamma t^{-(1+\lambda/6)} R^{1/3}$				
$\times \exp\{-\frac{1}{2}(\lambda/2)^{1/3}$				
$\times [R^{1/3} - (\ln t_0)^{1/3}]\}$	λ	0.34 ± 0.08	0.36 ± 0.08	0.65 ± 0.10
	t_0	4	4	4
	Γ ($10^{-2} \text{cm}^3/\text{g}$)	4.15 ± 0.06	4.37 ± 0.06	4.58 ± 0.10
	χ^2	1.4	1.3	2.2
Equation (4)	T_c (K)	2.7677	2.5547	2.2098
Power law		± 0.0005	± 0.0005	± 0.0007
$\Gamma t^{-\gamma}$	γ	1.089 ± 0.015	1.092 ± 0.010	1.126 ± 0.015
	Γ ($10^{-2} \text{cm}^3/\text{g}$)	5.04 ± 0.07	5.29 ± 0.06	5.41 ± 0.12
	χ^2	1.7	1.2	2.5

atmosphere from the melt using the Czochralski top-seeded solution technique.²³ This yields large, optically clear, single-crystal boules from which we cut the crystals. To obtain a constant demagnetization factor within each sample, the crystals were ground into sphere with diameters of 4–5 mm $\pm 0.1\%$.²² The Tb concentrations p were measured using three techniques: density measurements (comparing our measured crystal densities against the known densities of LiTbF_4 and LiYF_4), atomic absorption fluorescence spectroscopy, and Faraday rotation. The room-temperature Faraday-rotation measurements were made at a wavelength ($\lambda = 514.5$ nm) at which $\text{LiTb}_p\text{Y}_{1-p}\text{F}_4$ is transparent. A laser beam was passed through an optically polished disk of each crystal placed in a magnetic field. The Faraday-rotation of each crystal,

which is proportional to the number of magnetic ions, was then compared with that of the pure LiTbF_4 to obtain p .²⁴ The measured p 's for the eight crystals, along with their associated errors and their measured densities, are shown in Table I.

Previous experiments have shown that Tb^{3+} ions enter LiYF_4 substitutionally for the Y^{3+} ions with negligible lattice distortion. Low-temperature EPR measurements¹⁹ on the dilute $\text{LiTb}_{0.01}\text{Y}_{0.99}\text{F}_4$ have resulted in narrow linewidths and have been able to measure the g factor of the Tb^{3+} . This indicates that there is no rare-earth clustering in these very dilute crystals. Our own light scattering and Faraday-rotation measurements have proven that there is no rare-earth ion clustering on a macroscopic scale in our samples.

TABLE I. (Continued.)

0.63±0.015	0.46±0.015	0.375±0.015	0.24±0.015	0.155±0.020
4.92±0.01	4.66±0.02	4.53±0.03	4.32±0.05	4.19±0.05
$8 \times 10^{-4} < t < 10^{-1}$	$8 \times 10^{-4} < t < 10^{-1}$	$10^{-3} < t < 6 \times 10^{-2}$	$10^{-3} < t < 6 \times 10^{-2}$	
1.6645	1.1397	0.8186		
±0.0004	±0.0007	±0.0009		
0.30±0.07	0.13±0.07	0.06±0.01		
6.13±0.16	11.2±0.7	25±2		
3.9	13.0	11.7		
1.6648	1.1397	0.8181		
0.0004	0.0006	0.0007		
0.73±0.20	0.32±0.10	0.12±0.03		
7.0±0.2	12.9±0.7	31±3		
6.2	10.8	6.5		
1.6637	1.1379	0.8158	0.365	
±0.0003	±0.0003	±0.0007	±0.003	
0.81±0.04	1.40±0.08	2.52±0.24	6.0±1.2	
4	4	4	4	
5.42±0.06	7.28±0.14	8.8±0.9	14.5±4.0	
1.0	1.1	1.2	1.0	
1.6635	1.1379	0.8158	0.365	0.135
±0.0002	±0.0004	±0.0007	±0.003	±0.025
1.147±0.010	1.233±0.015	1.415±0.040	2.0±0.2	
6.32±0.08	8.1±0.2	9.2±1.0	14.5±4.0	
1.1	1.1	1.2	1.0	

B. ac susceptibility measurements

The magnetic ac susceptibility measurements were made using a mutual inductance bridge.²² The sample is placed in an external time varying homogeneous magnetic field. The susceptibility is then found with the bridge by measuring the voltage induced in a pickup coil by the time dependent magnetic moment of the sample. The bridge was calibrated to better than ±0.6% with a superconducting lead sphere. The bridge zero was obtained either by sample extraction or from a high-temperature Curie extrapolation of the susceptibility. Between extractions of the sample the bridge was stable to within ±0.001% and between runs the reproducibility was ±0.3%. The crystals were oriented with x rays and glued to the sample holders with their *c* axis oriented within two degrees of the direction of the applied magnetic field.

C. Cryogenics

To achieve the necessary temperatures, the five samples with $p \geq 0.46$ were immersed in pumped

liquid ⁴He. The $p=0.38$ crystal was immersed in pumped ³He and the $p=0.24$ and 0.155 crystals were thermally anchored to a copper block in contact with the mixing chamber of a He dilution refrigerator. The best experimental temperature regulation was achieved in the 0.46 and 0.63 crystals where the immersion ⁴He liquid is a superfluid and the temperature could be controlled typically to better than 10^{-4} K using an ac resistance bridge and an electrical heater. In the ³He and the normal ⁴He the temperature was regulated by varying the pumping speed of the liquid bath. Unfortunately, the critical temperature of the $p=0.79$ crystal fell in the temperature range just above the ⁴He lambda point, making it difficult to stabilize the temperature. Except in the refrigerator, the temperature of the sample was measured using a 33-Hz Kelvin bridge and a commercially calibrated carbon glass resistance thermometer. The thermometer calibration was checked against the ⁴He lambda point and the vapor pressure above the

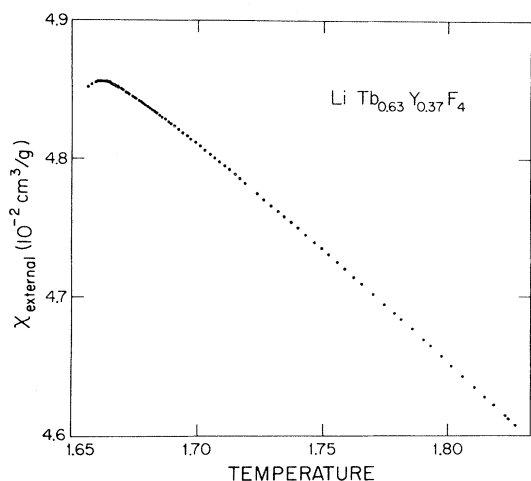


FIG. 2. The measured magnetic susceptibility χ_{ext} vs temperature of $\text{LiTb}_p\text{Y}_{1-p}\text{F}_4$ for the concentration $p=0.63$. The susceptibility has been divided by the density giving units of cm^3/g .

^4He . The thermometer, which was held about 4 cm from the sample and out of the pickup coils, was thermally anchored to the sample with a bundle of 40 AWG copper wires. In the dilution refrigerator,²⁵ located at the Naval Research Laboratory, the temperature was measured with a Speer carbon resistor thermally anchored to the copper block and calibrated during the run using the superconducting fixed point transitions of three NBS (National Bureau of Standards) calibrated superconductors.

V. ANALYSIS

In all eight of the crystals the measured peak magnetic susceptibility reached, within the precision of the inductance bridge, the value $1/N\rho$ (where $N=4\pi/3$ is the demagnetization factor for the spherical samples and ρ is the density in g/cm^3 for each sample). This value of the external susceptibility corresponds to an infinite internal susceptibility which occurs at a ferromagnetic phase transition. We conclude that the randomized $\text{LiTb}_p\text{Y}_{1-p}\text{F}_4$ exhibits a ferromagnetic transition at least for $p \geq 0.155$. Figure 2 shows the measured magnetic susceptibility χ_{ext} in the critical region for the concentration $p=0.63$.

The susceptibility measurements presented here were made with the inductance bridge operating at 100 Hz and with a 4-Oe peak modulated external

magnetic field. Some of the experiments were repeated at lower and higher field amplitudes in order to verify that there is no magnetic field dependence to our results. The experiments were also repeated at several frequencies. For each crystal the susceptibility at all temperatures above the temperature of the peak susceptibility is found to be independent of the frequencies used. Thus there is no frequency dependence to our critical phenomena results. Below the temperature of the peak susceptibility, the susceptibility decreases with decreasing temperature (see Fig. 2). For a given crystal this reduction with decreasing temperature is less severe at lower frequencies. Static (zero-frequency) susceptibility superconducting quantum-interference device (SQUID) measurements on $\text{LiTb}_{0.9}\text{Y}_{0.1}\text{F}_4$ show no falloff in susceptibility with temperature.²⁶ For any given frequency the falloff is more severe as p becomes smaller. We attribute this frequency- and temperature-dependent behavior to the formation of magnetic domains below T_c which have a resistance to movement on the time

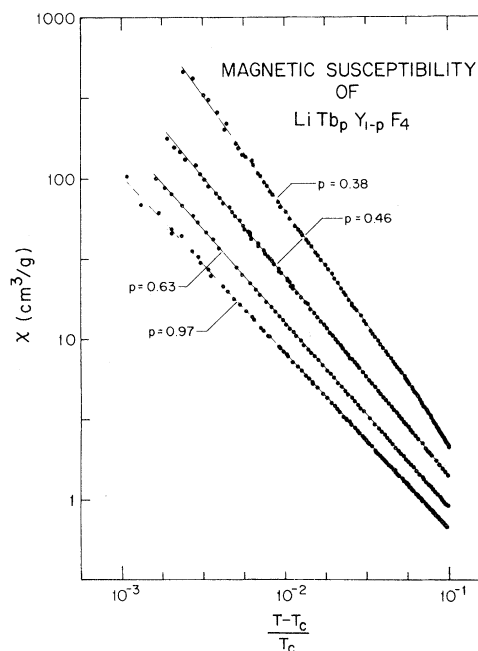


FIG. 3. Magnetic susceptibility χ vs reduced temperature t on logarithmic scales for four concentrations p of $\text{LiTb}_p\text{Y}_{1-p}\text{F}_4$. The solid lines are the fits to the power law Eq. (4). The close agreement between the data and the lines is illustrative of the low χ^2 values obtained from the Eq. (4) fits. The $p=0.38$ fit extends only to $t=6 \times 10^{-2}$. The susceptibilities have been corrected for demagnetizing effects according to Eq. (8).

scale of our driving frequencies. This resistance becomes more severe for the lower concentration crystals.

In order to analyze the data, the experimentally measured external susceptibility χ_{ext} was correlated for demagnetization effects to obtain the internal susceptibilities χ by using the decomposition formula

$$\chi^{-1} = \chi_{\text{ext}}^{-1} - N\rho. \quad (8)$$

Figure 3 shows our data for the four concentrations $p = 0.97, 0.63, 0.46,$ and 0.38 , and plots the internal susceptibility [corrected by Eq. (8)] versus t on logarithmic scales. Since the absolute calibration of the bridge is only accurate to $\pm 0.6\%$, we must scale the measured susceptibilities so that the peak value corresponds to exactly $1/N\rho$ and to $\chi^{-1} = 0$. If we allow this scale factor to vary as an adjustable parameter of the fits to the functional forms, the quality of the fit to each form is not affected. When this is done the adjustable parameter T_c becomes correlated with the scale factor. None of the other adjustable parameters is affected.

In order to test the appropriateness of each of the four functional forms Eqs. (1)–(4) to the data [Eq. (1b) is used in all of the fits], we have performed a nonlinear least-squares fit of each form to the data. The fitting procedure minimizes the parameter χ^2 given by

$$\chi^2 = \frac{1}{\sigma^2(n-f-1)} \sum_i [\chi_{\text{ext}}(t_i) - \chi_{\text{theor}}(t_i)]^2, \quad (9)$$

where n is the number of data points, f is the number of fitted parameters ($f = 3$ for all fits), σ is the estimated uncertainty in each measurement, and χ_{theor} is the theoretical functional form corrected by Eq. (8).

The measured magnetic susceptibility data for the seven crystals $p \geq 0.24$ were fitted to the four functional forms Eqs. (1b)–(4) and the results are given in Table I. The $p = 0.24$ concentration was only fitted to Eqs. (3) and (4). Temperature stabilization problems in the very low T_c , $p = 0.155$ crystal, presumably a result of the high heat capacity and a low heat conductivity of the samples near T_c , made it impossible to make high-resolution quantitative measurements. For this crystal we were only able to determine $T_c(p = 0.155) = 0.135 \pm 0.025$ K.

Owing to our finite experimental temperature resolution and to imperfections in the crystals, a

minimum practical limit in the measured reduced temperature used in the fits of the data ranged between 5×10^{-4} and 10^{-3} . The upper limit on the temperature range over which we fit was chosen by fitting the functional forms with an upper bound constrained so that it would not have a significant effect on the χ^2 of the fits. The reduced temperature range used for each concentration is shown in Table I. For each crystal the same range was used for each of the four fits in order to facilitate comparisons between the fits.

When comparing the χ^2 's of the fits in Table I, it should be realized that for each concentration the χ^2 's are normalized by the experimental uncertainty σ . Because the σ 's are not identical in all runs, it is difficult to compare the χ^2 's for each concentration with those of another concentration. We can compare the χ^2 's for different functional forms for each concentration.

A good fit of the data would result in a χ^2 value of 1. If we fit a function to the data and obtain a χ^2 near 1 we have not proven that this functional form is the true physical description of the data, but that over the fitted range the fit is consistent with the data. For example, previous susceptibility measurements in the pure crystals LiTbF_4 (Ref. 27) and LiHoF_4 (Ref. 28) testing Eq. (1) against Eq. (4) resulted in $\chi^2 \approx 1$ for both functional forms and were unable to distinguish between these forms. Other experiments,^{5–8} however, show with certainty that Eq. (1) was the proper description of the data.

VI. RESULTS

A. Critical phenomena

The χ^2 values for the fits of the $p = 0.97$ and 0.90 crystals shown in Table I are all between 1.2 and 1.7. Hence it is best to conclude that all of the four functional form equations (1)–(4) are possible candidates for the “appropriate” description of the susceptibility at these concentrations. We cannot conclusively distinguish between them. The $p = 0.79$ crystal has a slightly larger χ^2 (probably due to the awkward temperature range previously mentioned), but here again the relative χ^2 values for the four forms are not significantly different and we are unable to conclusively choose the appropriate form.

Examining the three concentrations $p = 0.63, 0.46,$ and 0.38 in Table I, we see that there is a marked difference in the relative χ^2 's for these fits. In particular, the χ^2 for the fits of both the non-

universal form equation (3) and the power-law equation (4) ranges between 1.0 and 1.2. This indicates an excellent agreement with the data.¹⁸ The χ^2 's for the asymptotic random form equation (2) for these three concentrations are 3.9, 13.0, and 11.7, respectively. These are all very poor fits to the data. Similarly, the pure form equation (1) results in χ^2 's of 6.2, 10.8, and 6.5, which also shows very poor agreement with the data. In these three medium concentration crystals the power-law and nonuniversal random susceptibility fits were quite insensitive to the portion of the reduced temperature range selected, and the fits always resulted in χ^2 values between 1.0 and 1.2. In contrast to this behavior, the fairly large χ^2 's obtained when fitting Eqs. (1) and (2) can be varied considerably by changing the reduced temperature range over which we fit. For example, for $p=0.63$ or 0.46 , if the maximum value of t is reduced from 10^{-1} to 3×10^{-2} , the χ^2 values are reduced but still conclusively show that form (1) and (2) are poor representations for the data. It is only for reduced temperature ranges smaller than one decade that the χ^2 values for the various functions become comparable. We conclude, therefore, that in the concentration regime $0.38 \leq p \leq 0.63$, neither the asymptotic random susceptibility equation (2) nor the pure RG susceptibility equation (1) can be considered to be an adequate description of the experimentally measured susceptibility.

A refinement has been proposed by Shalaev¹⁰ to the universal asymptotic random form equation (2) of Aharony. This refinement consists of multiplying Eq. (2) by the slowly varying logarithmic factor $(\ln t)^{-w}$. For the four-dimensional short-range Ising model $w \approx 0.37$, but w has not been calculated for the three-dimensional dipolar case studied here. Fitting with this correction term included in Eq. (2) in the $p=0.63$ and 0.46 concentrations resulted in even poorer fits than with the uncorrected Eq. (2) for all $w > 0$. We conclude then that the corrected asymptotic form cannot adequately describe the data for $p \leq 0.63$.

Forms (1) and (2) were also shown to be poor fits for the $p=0.24$ concentration crystal. The fits are not shown in Table I because the statistics were fairly poor. In measuring the susceptibility of a crystal with $p=0.32$ Beauvillain *et al.*¹⁴ have obtained results similar to ours.¹⁸ In the lowest concentration crystals, especially $p=0.46$ and 0.38 , the t_0 adjustable parameter in the random form equation (2) fit becomes dependent on the upper bound t_{\max} of the reduced temperature range over which

it is fit. In each fit, t_0 adjusts to just larger than the t_{\max} chosen and is thus not a property of the crystal. Without the adjustable parameter t_0 in the Eq. (2) fits (i.e., if we set $t_0=1$), the χ^2 rises drastically, showing a large discrepancy between Eq. (2) and the data for all seven concentrations.

In fitting the nonuniversal crossover region susceptibility equation (3) predicted to be appropriate in the region $t_x \ll t \ll 1$, we have allowed the amplitude Γ to vary in each fit but we have kept the parameter t_0 fixed at the measured pure value of 4.0. All four of our functional forms then have exactly three adjustable parameters (Γ , T_c , and either γ , t_0 , or λ).

In Table I we see that Eq. (3) fits all of the concentrations with a χ^2 equal to or better than the best fit for any of the other three forms and that χ^2 is always close to 1 (except the anomalous $p=0.79$ previously discussed). As mentioned before, this is due to the similarity between Eq. (3) and the pure RG form equation (1) near $p=1$ and between Eq. (3) and the power-law equation (4) for $p \leq 0.63$. These agreements provide evidence for the appropriateness of this nonuniversal form equation (3) in describing our data.

For small $1-p$, the Γ amplitude in Eq. (3) should not have any explicit p dependence. Table I shows that for $0.79 \leq p \leq 0.97$ there is a slight p dependence and that for $p \leq 0.63$ there is a fairly large p dependence in Γ . The calculation for Eq. (3) also predicts for small $1-p$ a dependence $\lambda \propto (1-p)^3$. This relationship is not found to be consistent with our data. It is possible, however, that if these relationships are true that they only hold for $p \gtrsim 0.9$ where our data cannot conclusively test them.

Since the crossover temperature has the functional dependence $\ln t_x \propto -[p(1-p)]^{-3}$, we expect that if we were near the asymptotic temperature regime, the rise in t_x would cause the universal random equation (2) to fit the data better rather than worse as p decreases from one. Our experimental results indicate that with the more dilute crystals $0.24 \leq p \leq 0.63$, we have a poor agreement between Eq. (2) and the data in the experimentally accessible temperature range $10^{-3} < t < 10^{-1}$. We conclude that our experimental temperatures are not in the asymptotic temperature range for any concentration of $\text{LiTb}_p\text{Y}_{1-p}\text{F}_4$.

The crossover behavior of random dipolar-coupled Ising ferromagnets has recently been studied by Liebmann *et al.*^{29,30} using numerical techniques. They have concluded that the crossover re-

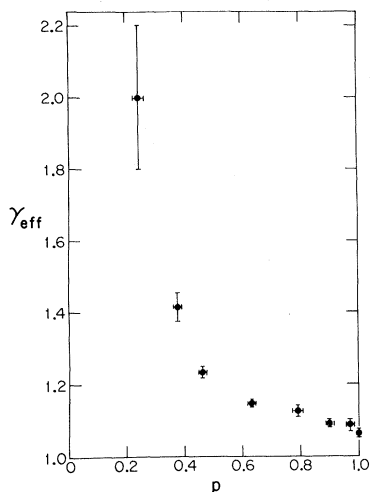


FIG. 4. Effective exponent γ vs magnetic concentration p in $\text{LiTb}_p\text{Y}_{1-p}\text{F}_4$. γ is obtained by fitting Eq. (4) to the data for each concentration. The $p=1$, $\gamma=1.06$ value is from Refs. 26 and 30.

gion separating the “pure” behavior equation (1) from the “random” behavior equation (2) is actually extremely broad and extends over many decades in reduced temperature. Thus the numerical work of Liebmann *et al.* is in complete agreement with our conclusion that the experimentally accessible temperature range is not near the asymptotic region of the universal random form equation (2).

B. γ vs p

The solid lines in Fig. 3, which represent the power-law fits [Eq. (4)], indicate that there is a good agreement between the data and a simple power law. In Fig. 4 the effective critical exponents γ obtained from fitting Eq. (4) are plotted as a function of p . The pure $p=1$ exponent has been measured at 1.06,^{27,30} which is close to the classical result, $\gamma=1$. The small discrepancy of 0.06 between these values occurs because our measurements are not made in the asymptotic temperature range. The $\ln(t_0/t)^{1/3}$ correction term in Eq. (1b) causes the exponent γ in Eq. (4) to be temperature dependent, and in the range $10^{-3} < t < 10^{-1}$ with $t_0=4$ we can calculate $\gamma=1.060$.²²

From Fig. 4 we see that γ is concentration dependent. For lower concentrations γ rises rapidly reaching 2.0 at $p=0.24$ and giving the appearance of diverging at some low concentration. Previous high-temperature series-expansion studies³¹ of the short-range Ising magnet have shown a concentration dependent γ which qualitatively is similar

to the behavior shown in Fig. 4. An RG calculation by Kawasaki³² for the short-range case has found that critical exponents may change due to the existence of a correlation in the random occupation of sites. Stephen and Aharony¹³ have suggested that the short-range percolation critical region is broadened by the presence of the long-range forces and that the increase in γ is a manifestation of finite temperature precolation exponents.

In order to characterize the $\gamma(p)$ dependence, the phenomenological equation $\gamma(p)=1.06pT_c(1)/T_c(p)$ has been proposed.^{14,22} The 1.06 factor is included to correct for the nonasymptotic temperature range of the measurements. The $\gamma(p)$ values predicted from this formula are in excellent agreement with our $\gamma(p)$ measurements.

C. T_c -vs- p phase diagram

The T_c 's for each of our eight concentrations are plotted in Fig. 5. Figure 5 also includes the pure point $T_c(p=1) = 2.88$ K.^{5-8,15,17,27} The $T_c(p)$ data appears quite straight and has been least-squares fit with a linear line constructed to pass through the pure T_c . This line is shown in Fig. 5 and can be represented with the equation

$$T_c(p)/T_c(1) = 1 - (1.137 \pm 0.025)(1-p). \quad (10)$$

By extrapolating this line to zero temperature we obtain an “apparent” percolation concentration of $p_c = 0.12 \pm 0.02$. We do not know whether the $T_c(p)$ phase line remains linear below the lowest data point $T_c(0.155)/T_c(1)=0.05$ and if there is a

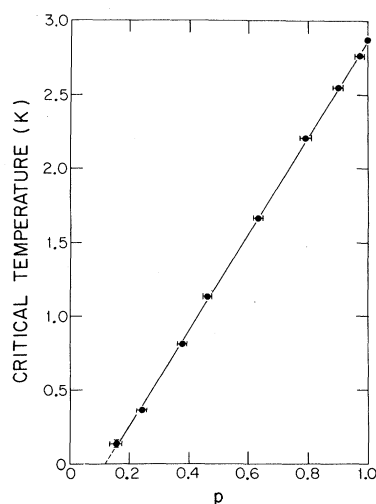


FIG. 5. Critical temperature T_c vs magnetic concentration p in $\text{LiTb}_p\text{Y}_{1-p}\text{F}_4$. The solid line is a least-squares fit to the data. The $p=1$, $T_c=2.88$ K value is from Refs. 4–9 and 26.

true percolation. Short-range site dilution calculations for $dT_c(p)/T_c(1)dp$ near $p=1$ give values between 1.02 and 1.20 (Ref. 12) (which are close to our measured dipolar value). Short-range calculations for p_c of a four nearest-neighbor crystal lattice range between 0.33 and 0.59.¹² This is much larger than our extrapolated p_c .

According to the mean-field ground-state splitting calculation, the $T_c(p)$ phase line should bend over and go to a $p_c \approx 0.23$.^{20,22} The data are not in agreement with this prediction; the data clearly indicate ferromagnetism for $p \geq 0.155 \pm 0.020$. The mean-field splitting calculation predicts nonlinear behavior for $T_c(p)$ at low concentrations, whereas our $T_c(p)$ data appear to be quite linear. The dilute dipolar-coupled $T_c(p)$ prediction equations (5) and (7) do not take the splitting into account.

In order to compare the predictions Eqs. (5) and (7) with our data it is necessary to calculate a lattice sum of $\tanh(J/kT)$. The sum is performed by using the Lorentz approximation where we exactly sum all of the Tb or Y sites within a small sphere (diameter = 350 Å) and then integrate over the remaining volume. The summation is performed in an infinitely long cylinder so that the demagnetizing field is zero (i.e., $h_{\text{int}} = h_{\text{ext}}$). To match the condition that $T_c(p=1) = 2.88$ K in Eq. (7) the parameter S was varied, and in Eq. (5) the entire sum was multiplied by a constant. Unfortunately, performing these sums and calculating the $T_c(p)$ phase line with both Eqs. (5) and (7) we find that these predictions do not vary significantly from the linear mean-field behavior $T_c(p) = pT_c(1)$. In Fig. 6 the low p results of the calculation of the replica method prediction Eq. (6) are shown (dashed line) along with our data and the least-squares fit to our data (solid line). As can be seen in Fig. 6, although the low- p T_c predictions do vary slightly

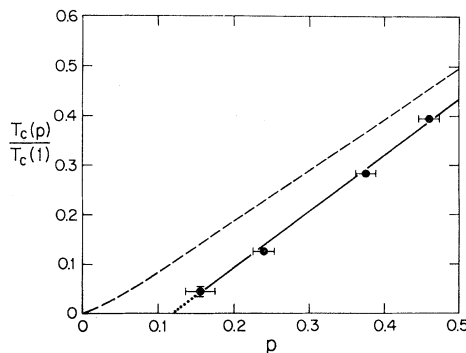


FIG. 6. The $T_c(p)$ phase line of $\text{LiTb}_p\text{Y}_{1-p}\text{F}_4$. The dashed line is $T_c(p)$ calculated using Eq. (5). The solid line is a linear fit to our data.

from a mean-field behavior, it is not nearly enough so that we could say that either of these predictions can adequately describe our data.

Stephen and Aharony¹³ also predicted that when the condition

$$\sum_i (\tanh J_{ij}/kT)^2 > \sum_i (\tanh J_{ij}/kT) \quad (11)$$

holds, that there might be a transition to a spin-glass state. We calculate that this condition is met in the LiTbF_4 crystal structure for $p < 0.10$. It is not clear how to interpret this in light of the failure of the theory to predict $T_c(p)$ and the somewhat interesting coincidence that our extrapolated p_c is close to this value.

VII. CONCLUSIONS

This paper has presented measurements of the magnetic susceptibility and $T_c(p)$ phase diagram in the random dipolar-coupled Ising ferromagnet $\text{LiTb}_p\text{Y}_{1-p}\text{F}_4$ in the range $0.97 \geq p \geq 0.155$. The magnetic susceptibility has been compared to the pure susceptibility function equation (1b), the random susceptibility equation (2), the “nonuniversal” random function equation (3), and to the conventional power-law form equation (4). In the $p = 0.97$ and $p = 0.90$ crystals it is not possible to quantitatively distinguish between these four forms. In the $p = 0.63, 0.46,$ and 0.38 crystals, Eqs. (3) and (4) yield lower χ^2 values than Eqs. (1b) or (2). The effective nonuniversal critical-point exponents obtained by fitting Eq. (4) are concentration dependent and appear to diverge at small values of p . The above results, in conjunction with the numerical calculations of Liebmann *et al.*, indicate that the asymptotic temperature range in which Eq. (2) is valid has not been attained in $\text{LiTb}_p\text{Y}_{1-p}\text{F}_4$.

The $T_c(p)$ phase line was determined to be linear in p with a slope $dT_c(p)/T_c(1)dp = 1.137 \pm 0.025$ K, which extrapolates to a percolation concentration $p_c = 0.12 \pm 0.02$. This nonzero p_c is not predicted using either of the calculations for dipolar-coupled magnets, Eqs. (5) or (7). A mean-field non-Ising split ground-state calculation predicts a $p_c = 0.23$.^{20,22} It is possible that the existence of ferromagnetism below the $p_c = 0.23$ percolation concentration predicted by the ground-state splitting calculation is due to a cooperative nuclear electronic spin interaction.^{33,34} This “enhanced” nuclear spin ordering is predicted to occur at the approximate temperature

$$T_c \approx p \sum J(A/\Delta)^2 \left[1 - 2 \sum J/\Delta \right]^{-1},$$

where A/Δ is the ratio of the hyperfine interaction to the ground-state splitting.³⁴ The large hyperfine interaction in $\text{LiTb}_p\text{Y}_{1-p}\text{F}_4$ [$A=0.3$ K (Ref. 19)] results in a predicted $p=0.15$ transition temperature of $0.08-0.10$ K for the nuclear ferromagnetism. This is not far from our measured $T_c=0.135$ K.

Additional experiments with $p < 0.15$ would be helpful in establishing the existence of this nuclear-electronic spin ordering, to look for any possible percolation transition, or to look for a spin-glass state.

ACKNOWLEDGMENTS

We would like to thank D. Gabbe for growing the $p=0.46$ and 0.97 crystals and M. Huster for growing the $p=0.79$ and 0.90 crystals. We are grateful to M. Huster, S. Brierley, and B. Romanow for experimental assistance as well as to C. Vause, T. C. Lubensky, and A. B. Harris for numerous discussions. This work was supported by the National Science Foundation under Grant No. DMR-77-23409, by NSF Materials Research Laboratory DMR-76-80994, and by the Research Corporation.

*Present address: Xerox Corp., Joseph C. Wilson Center for Technology, Rochester, N. Y. 14644.

¹A. B. Harris, *J. Phys. C* **7**, 1671 (1974).

²A. B. Harris and T. C. Lubensky, *Phys. Rev. Lett.* **33**, 1540 (1974); T. C. Lubensky, *Phys. Rev. B* **11**, 3573 (1975); G. Grinstein and A. Luther, *ibid.* **13**, 1329 (1976); D. E. Khmel'nitskii, *Zh. Eksp. Teor. Fiz.* **68**, 1960 (1975) [*Sov. Phys.—JETP* **41**, 981 (1976)].

³M. E. Fisher, *Rev. Mod. Phys.* **46**, 597 (1974); S. K. Ma, *Modern Theory of Critical Phenomena* (Benjamin, Reading, Mass., 1976).

⁴A. I. Larkin and D. E. Khmel'nitskii, *Zh. Eksp. Teor. Fiz.* **56**, 2087 (1969) [*Sov. Phys.—JETP* **29**, 1123 (1969)]; A. Aharony, *Phys. Rev. B* **8**, 3363 (1973); A. Aharony and B. I. Halperin, *Phys. Rev. Lett.* **35**, 1308 (1975); E. Brezin and J. Zinn-Justin, *Phys. Rev. B* **13**, 251 (1976).

⁵G. Ahlers, A. Kornblit, and H. J. Guggenheim, *Phys. Rev. Lett.* **34**, 1227 (1975).

⁶J. Als-Nielsen, *Phys. Rev. Lett.* **37**, 1161 (1976).

⁷J. A. Griffin, J. D. Litster, and A. Linz, *Phys. Rev. Lett.* **38**, 251 (1977); J. A. Griffin and J. D. Litster, *Phys. Rev. B* **19**, 3676 (1979); J. A. Griffin, M. Huster, and R. J. Folweiler, *ibid.* **22**, 4370 (1980).

⁸R. Frowein, J. Kotzler, and W. Assmus, *Phys. Rev. Lett.* **42**, 739 (1979).

⁹A. Aharony, *Phys. Rev. B* **13**, 2092 (1976).

¹⁰B. N. Shalaev, *Zh. Eksp. Teor. Fiz.* **73**, 2301 (1977) [*Sov. Phys.—JETP* **46**(6), 1204 (1977)].

¹¹C. Vause and J. Bruno, *Phys. Lett.* **81A**, 291 (1981).

¹²S. K. Ghatak, *J. Phys. C* **11**, 1401 (1978); A. Aharony, *J. Magn. Magn. Mater.* **7**, 198 (1978); M. F. Thorpe and A. R. McGurn, *Phys. Rev. B* **20**, 2142 (1979).

¹³M. J. Stephen and A. Aharony, *J. Phys. C* (in press).

¹⁴P. Beauvillain, J. Seiden, and I. Laursen, *Phys. Rev. Lett.* **45**, 1362 (1980); P. Beauvillain, C. Chappert, J. P. Renard, and J. A. Griffin, *J. Phys. C* **13**, 395 (1980).

¹⁵L. M. Holmes, T. Johansson, and H. J. Guggenheim, *Solid State Commun.* **12**, 993 (1973).

¹⁶H. P. Christensen, *Phys. Rev. B* **17**, 4060 (1978).

¹⁷L. M. Holmes, J. Als-Nielsen, and H. J. Guggenheim, *Phys. Rev. B* **12**, 180 (1975); J. Als-Nielsen, L. M. Holmes, F. K. Larsen, and H. J. Guggenheim, *ibid.* **12**, 191 (1975); J. Als-Nielsen, L. M. Holmes, and H. J. Guggenheim, *Phys. Rev. Lett.* **32**, 610 (1974).

¹⁸J. A. Griffin, J. J. Folkins, and D. Gabbe, *Phys. Rev. Lett.* **45**, 1887 (1980).

¹⁹I. Laursen and L. M. Holmes, *J. Phys. C* **7**, 3765 (1974).

²⁰R. J. Birgeneau, in *Magnetism and Magnetic Materials—1972 (Denver)*, Proceedings of the 18th Annual Conference on Magnetism and Magnetic Materials, edited by C. D. Graham and J. J. Rhyne (American Institute of Physics, New York, 1972), p. 1664.

²¹R. J. Elliot, P. Pfeuty, and C. Wood, *Phys. Rev. Lett.* **25**, 443 (1970); A. P. Young, *J. Phys. C* **8**, L309 (1975); R. J. Elliot and C. Wood, *ibid.* **4**, 2359 (1971).

²²J. J. Folkins, Ph.D. thesis, University of Pennsylvania, 1981 (unpublished).

²³D. Gabbe and A. L. Harmer, *J. Cryst. Growth* **3**, 4 (1968).

²⁴M. J. Weber, R. Morgret, S. Y. Leung, J. A. Griffin, D. Gabbe, and A. Linz, *J. Appl. Phys.* **49**, 3464 (1978); J. A. Griffin, J. Folkins, M. J. Weber, R. Morgret, J. D. Litster, D. Gabbe, and A. Linz, *ibid.* **49**, 2209 (1978).

²⁵D. U. Gubser and L. D. Jones, *Rep. NRL Prog.* June 1971.

²⁶S. K. Brierley, J. A. Griffin, and C. A. Vause, *Solid State Commun.* (in press).

²⁷P. Beauvillain, C. Chappert, and I. Laursen, *J. Phys. C* **13**, 1481 (1980).

²⁸P. Beauvillain, J. P. Renard, I. Laursen, and P. J. Walker, *Phys. Rev. B* **18**, 3360 (1978).

²⁹R. Liebmann, B. Schaub, and H. G. Schuster, *Z. Phys.* **B 37**, 69 (1980).

³⁰J. Kotzler, H. Reinhardt, R. Liebmann, and H. G.

- Schuster, Phys. Rev. B 23, 1476 (1981).
- ³¹T. Oguchi, J. Phys. Soc. Jpn. 26, 580 (1969); T. Idogaki and N. Uryu, *ibid.* 43, 845 (1977); M. Suzuki, J. Phys. C 7, 255 (1974).
- ³²T. Kawasaki, Progr. Theor. Phys. 55, 1016 (1976).
- ³³K. Andres, Phys. Rev. B 7, 4295 (1973).
- ³⁴T. Murao, J. Phys. Soc. Jpn. 31, 683 (1971); T. Murao, *ibid.* 33, 33 (1972).